# Performance Analysis of a Small-Scale Photovoltaic Water Pumping System

Montana Rungsiyopas[1] and Chokchai Chuenwattanapraniti[2*]
[1] Department of Mechanical Engineering, Faculty of Engineering, Burapha University Chonburi 20131, Thailand
[2] Department of Electrical Engineering, Faculty of Engineering, Burapha University Chonburi 20131, Thailand
*Corresponding author: chokchai@eng.buu.ac.th

*Received : 28 March 2022 / Revised 1st: 24 May 2022 / Revised 2nd : 27 May 2022 / Accepted : 28 May 2022*

***Abstract*** The performance of a photovoltaic (PV) pumping system depends on several factors such as the pump head, PV array size, and solar radiation. This research aims to investigate and analyze the performance of a small PV pumping system driven by an AC motor under various system configurations and solar irradiance. The 1.1 kW motor coupled to the surface pump was then formulated in the laboratory and the test results were carried out under different testing conditions. The polynomial regression was applied to the test data providing the empirical model relating the water flow rate and head for each solar irradiance. In the estimation of daily water delivery, some examples of solar irradiance profiles were entered into the model. In addition, performance analysis was performed which enables the selection of proper system configulation to fulfill the daily water demand while achieving high system efficiency.

***Keywords***: PV pumping system, Solar irradiance, Surface pump, Pump performance.

## 1. Introduction

Nowadays, PV modules are widely used as a power source for several applications but one most benefit in use is the water pumping system especially in remote area. In developing countries, the water supplied for irrigation, agriculture and cattle are important and worth especially in rural areas lacking of utility electric grid. Therefore, the photovoltaic pumping system is an attractive choice in such area [1-2]. The simple PV pumping system may consist of PV array directly connected to DC motor pump. However, most of the latest technologies include the pump controller for performance improvement purpose. In potable water supply needs the positive displacement pump in order to overcome the high head loss while in irrigation and

agriculture use centrifugal pump to cover the massive flow rate.

In the past research, many researchers [3-6] studied the performance of a pumping system that connects the PV array directly coupled to DC motor-pump without batteries. They [3-5] developed the model consisted of two mathematic functions: the I-V characteristic for both PV array and DC motor-pump, Q-V characteristic for motor-pump. These models predict the flow rate at any solar irradiance and water head. The effect on pumping head on solar pumping system using the optimum PV array was also investigated [7]. There is also a development of sizing chart for a low cost positive displacement pump driven by DC motor based on field testing data [8].

For a constant input power and at low head up to 20 m, centrifugal pumps produce the greater water pumped per day than positive displacement pumps [9]. Therefore, the centrifugal type was widely used as surface pump for water lifting from shallow wells such as agricultural water pumping system and irrigation water supply application. Generally, most of centrifugal pumps are driven by AC motors which have more reliable and lower maintenance cost than DC type [10]. The main drawback of DC motors is that they require a frequent brush replacement consequently increasing running cost [11, 12]. Furthermore, in developing countries, the motor-pump rating over 1 kW which can generally be purchased is the AC type. In case of AC motor, a VFD (or solar pump inverter) needs to be placed between PV array and motor for the energy conversion purpose. Most of VFDs [13, 14] traditionally operate on V/F principle which maintains constant air-gap flux density so that maximize the torque per ampere. For the past several years, many researchers concerned in improving control strategies to enhance the pumping performance [15, 16]. Anyway, the system performance can also be upgraded by an optimized array size matching to the insolation and pumping head [17]. Considering only each component's characteristics to estimate water delivery is not accurate because system yields depend on the system's operating conditions, such as solar radiation, array size, pumping head, and the system efficiency [18]. Consequently, this paper focuses on the performance analysis of a small PV pumping system employing the experimental data to indicate the optimum system satisfying both water delivery requirements and system efficiency.

## 2. Pumping Test Rig and Setting of Experiment

The PV pumping system was designed to simulate the real operating condition. The data acquisition system was also installed to collect the flow rate, solar insolation, differential pressure, voltage, current, and power. The layout and photographs of simulated PV

pumping and data acquisition system is shown in Fig. 1 and Fig. 2.

### 2.1 Photovoltaic water pumping system

The photovoltaic water pumping test facility consists of a centrifugal pump, an AC motor, an inverter, and photovoltaic array. The technical specifications of all major components are shown in Table 1.

The PV array was tilted 13 degrees, which is the latitude of Burapha University, and faced to the south as shown in Fig. 3. The 1.1 kW motor-driven centrifugal pump was used in research and it can provide the flow rate which range between 10-450 l/min. The 1.15 kW solar pump inverter was selected to match the motor' s rated current and power. The inverter can function either as the normal VSD or the solar pump controller. In the latter, the PV array must be directly connected to the DC bus terminal of inverter.

**Table 1** Technical Specifications Summary of the Photovoltaic Water Pumping System

| | | |
|---|---|---|
| Pump | Type | centrifugal pump |
| | Model | Venz VC150 |
| | Head(max/min) | 28 m/5 m |
| | Design flow rate | 10-450 l/min |
| | Maximum pressure | 6 bars |
| | Input/output port | 2-inch/2-inch |
| | Materials | Cast iron body, Brass impeller |
| Motor | Type | Three-phase induction motor |
| | Model | Venz VC150 |
| | Rated voltage | 220-240V (Δ) |
| | Rated current | 4.4 A |
| | Rated power | 1.5HP/1.1 kW |
| | Frequency | 50 Hz |
| | Maximum speed | 3000 rpm |
| Inverter | Type | Solar pump inverter |
| | Model | ABB ACS-355 01E-07A5-2+N827 |
| | Input voltage | 150-400VDC |
| | Rated input current | 17 A |
| | Rated output voltage | V/F control |
| | Rated output current | 7.5 A |
| | Rated output power | 1.15 kW |
| | Output frequency | 0 to 599 Hz |
| PV | Type | Polycrystalline silicon |
| | Model | SUNTECH STP290-24Ve |
| | Maximum power | 290 $W_p$ |
| | Module efficiency | 14.9% |
| | $V_{mpp}$ | 35.6 V |
| | $I_{mpp}$ | 8.15 A |
| | $V_{oc}$ | 45.0 V |
| | $I_{sc}$ | 8.42 A |
| | Dimensions | 1956mm×992mm×40mm |

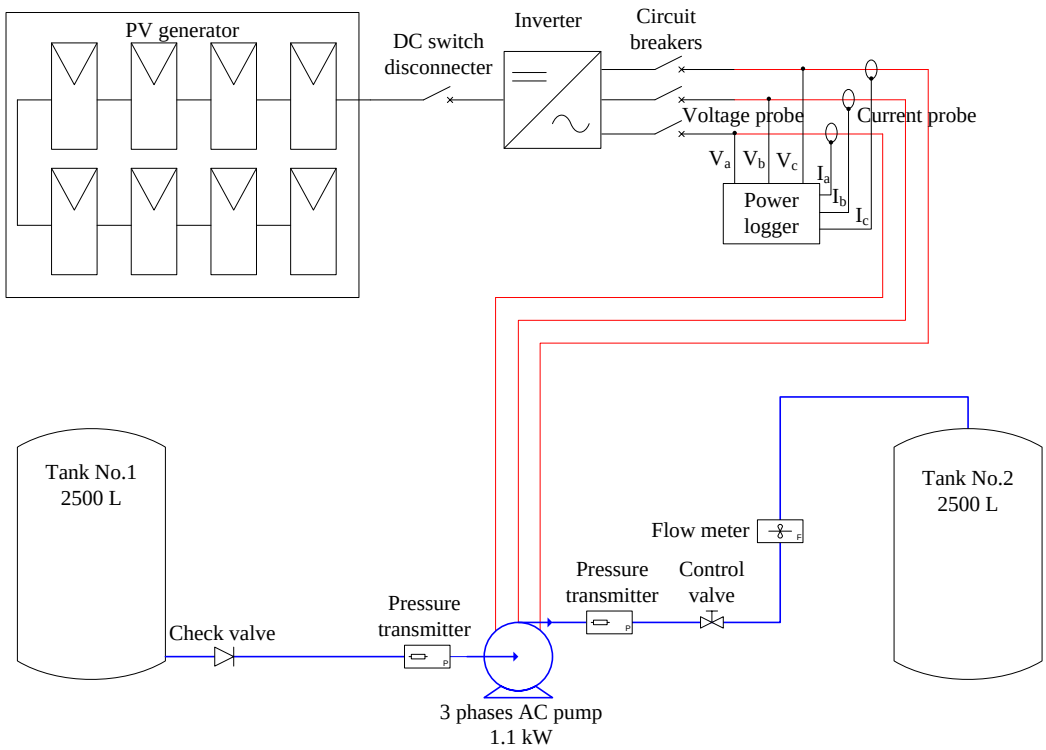


**Fig.1**. Schematic diagram of the PV water pumping system and data acquisition system

**Fig.2**. Water pumping system at the ground floor

### 2.2 Measuring equipment and devices

#### 2.2.1 Magnetic flow meter

A Yokogawa magnetic flow meter model AXF040G was used for volumetric flow measurement. The operation of this type of flow meter is based on Faraday's law so that it doesn't have any moving parts. This device is commonly ideal for applications where low pressure drop and low maintenance are required. The output signal is 4 - 20 mA. The measurable flow rate range is 0 - 45.23 $m^3/h$ with nominal accuracy ±0.35% of rate. However, the minimum readable flow rate is limited about 10% of maximum predefined flow.

#### 2.2.2 Pressure transducer

Two Trafag type 8472.26.5717 pressure transducers with accuracy ±0.5% were applied to measure the pressure drop across the control valve which is manually adjusted to simulate variable water head. The output signal is 4 - 20 mA, corresponding to pressure 0 bar to 4 bars. The pressure drop was converted into friction head and then summed it up with static head in order to evaluate the total head.

#### 2.2.3 Pyranometer

Kipp and Zonen SP-Lite pyranometer with sensitivity of 8.2 $\mu V/W.m^{-2}$ was mounted in the same angle as PV panels to monitor global tilted solar irradiance, also called Plane of Array (POA) irradiance.

#### 2.2.4 Power analyzer

PV voltage, current, and power on DC side of inverter were collected by a Yokogawa power analyzer model WT310 while voltage, current, power, and power factor at the motor-pump terminal were gathered by a Metrel power analyzer model MI-2892 which enables for measurement invariable speed drive application.

#### 2.2.5 Thermocouple

Two thermocouples of type K were used to measure ambient air temperature and water temperature in the tank.

#### 2.2.6 Data logger

All instantaneous measured signals: volume flow rate, pressure drop, solar irradiance, and temperature were recorded by a data logger Yokogawa model GP10.

**Fig.3**. Photovoltaic array at the rooftop of building

### 2.3 Operation principle and set-up the solar pump inverter

The main task of solar pump inverter is to convert the DC power from PV array to AC power for driving motor pump unit. With the latest technology, it will normally accompany with maximum power point tracking (MPPT) algorithm in order to extract maximum power from the PV array at any conditions. This is achieved by the well-known "Constant V/F (flux)" control. The output frequency of inverter is varied depending on the solar irradiance level until the maximum power point operation is reached. However, to maintain air-gap flux density affecting the torque performance of induction motor, the voltage magnitude must be changed in such a way that V/F ratio are maintained as shown in Fig. 4.

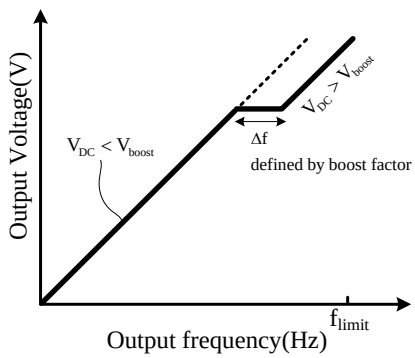


**Fig.4**. V/F pattern

**Table2** Parameters for inverter setting

| Parameter | Set-up value |
|---|---|
| **Control mode** | V/F (Pump control) |
| **Start/Stop input** | Auto |
| **Start DC voltage** | 150 V |
| **Maximum PV voltage** | 380 V |
| **Pump maximum speed** | 3000 rpm |
| **Boost voltage** | at nominal $V_{mpp}$= 35.6V/Module |
| **Boost factor** | 1.0(disable)/1.05/1.1 |
| **Motor parameter** | Nominal voltage 220 V<br>Nominal power 1.1 kW<br>Nominal current 4.4 A<br>Nominal speed 2950 rpm |

Table 2 shows the important parameters concerned in inverter setting. The inverter was set in "Auto Mode" so it does not need any manual start/ stop input. It starts automatically when DC input voltage is more than the "Start DC voltage" . To prevent the motor from stalling, the starting DC voltage was defined at 150 V.

The "Boost Factor" enables increasing the pump speed by increasing inverter output frequency when the actual PV voltage is greater than the "Boost Voltage". In case of small number of PV module in series (low DC bus voltage), the maximum power operating point will not achieve due to the limitation of constant V/F rule. "Boost Factor" allows the inverter output frequency to be increased by a predefined boost factor even if the output frequency does not agree to constant V/F. In the experiments, the "Boost Factor" was set to 1.0 (disable), 1.05 and 1.1 respectively while the "Boost Voltage" was set at nominal voltage at maximum power point (Vmpp) of PV array.

## 3. METHODOLOGY

Generally, the PV pumping performance depends on two main parameters; solar irradiance and water head. It is necessary to develop a system model that will be employed to predict the flow rate for any solar irradiance and head. The modelling procedure will be described as follow.

Firstly, at a constant solar irradiance, the instantaneous flow rate (Q) for differently simulated head (H) was collected. For the 2.32 kWp array (8 modules in series) which is around two times pump's rated power, the measured flow rate were plotted versus head and their fitting curves were also illustrated in Fig. 5. The maximum flow rate was approximately 300 l/min which was obtained at 3 m head and 1000 W/m$^2$ solar irradiance. At this condition, the motor input current and power were nearly its nominal value. Therefore, the boost factor was disable in this case.

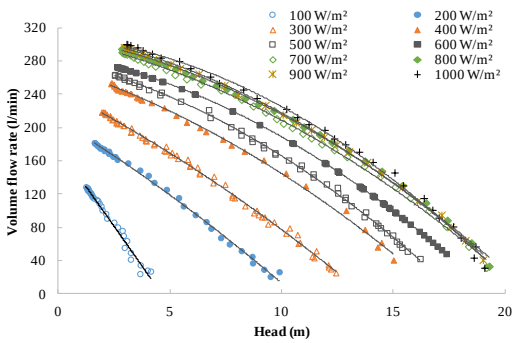


**Fig.5**. Flow rate vs. Head characteristics at various solar irradiance for 2.32 kW$_p$ array power (without boost factor)

The performance evaluation for 6 modules in series which provides 1.5:1 ratio between array and pump power was also investigated and the result was shown in Figure 6. For this PV configuration, the maximum water flow rate was around 200 l/min while the power measured at motor terminal was 450 W and the DC voltage at PV terminal was 224 V. From the PV module's specification shown in Table 2, the voltage at maximum power point ($V_{mpp}$) is 35.6 V per modules which will be 213 V for array consisted of 6 modules. The higher operating voltage than $V_{mpp}$ indicates that the PV array operates on the right side of array maximum-power-point. In order to shift the operating point to maximum-power-point, the boost factor was introduced at two predefined values 1.05 and 1.1 respectively. The effect of boost factor in pumping performance enhancement is obviously seen in Figs. 7 and 8. The Q-H curves were raised up especially for high irradiance and it can be observed 5-10% increasing in water flow rate.

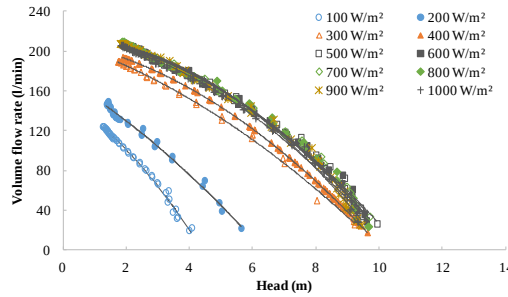


**Fig.6**. Flow rate vs. Head characteristics at various solar irradiance for 1.74 kW$_p$ array power (without boost factor)

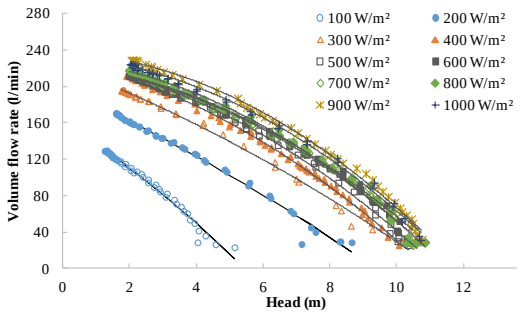


**Fig.7**. Flow rate vs. Head characteristics at various solar irradiance for 1.74 $kW_p$ array power (With 1.05 Boost Factor)

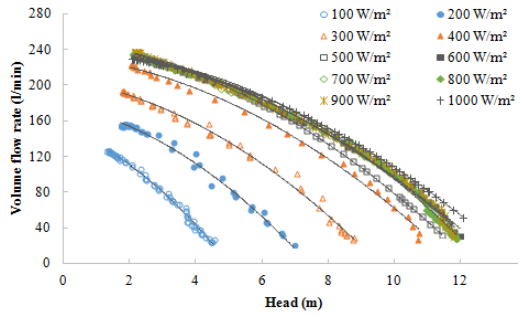


**Fig.8**. Flow rate vs. Head characteristics at various solar irradiance for 1.74 $kW_p$ array power (With 1.1 Boost Factor)

The next step is to develop a function relating the flow versus head from collected data. For each constant irradiance curve shown in Figs. 5 – 8, the second-order polynomial described the flow rate to head are defined as

$$Q\ H\ \big|_{G=const.} = a + bH + cH^2 \qquad (1)$$

Each corresponding coefficient of regressions (a, b, c) as defined in Eq. (1) can be determined by polynomial regression. The dot markers shown in Figs. 9 – 12 deal with the coefficients a, b and c related to each solar irradiance (G) for different array configurations.

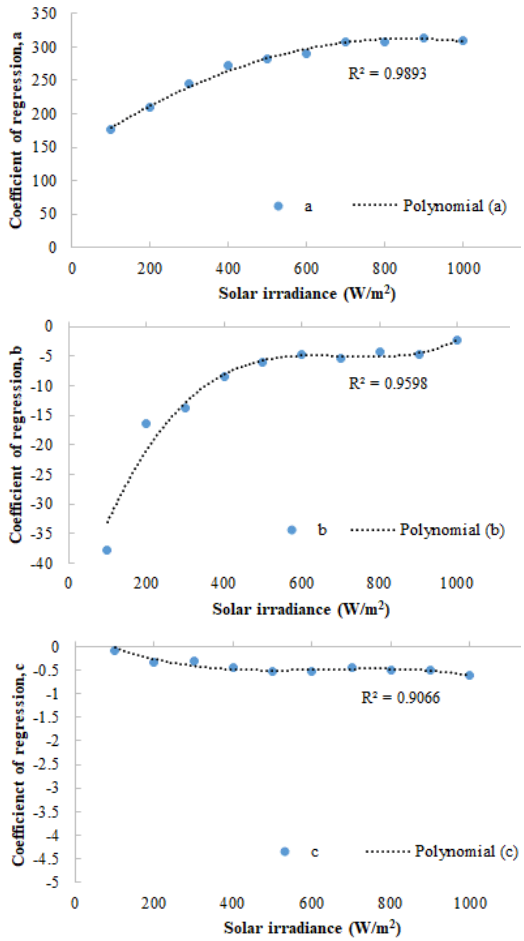


**Fig.9**. The relation between coefficient of regressions a, b, c and solar irradiance (G) for 2.32 $kW_p$ array power (without Boost Factor)

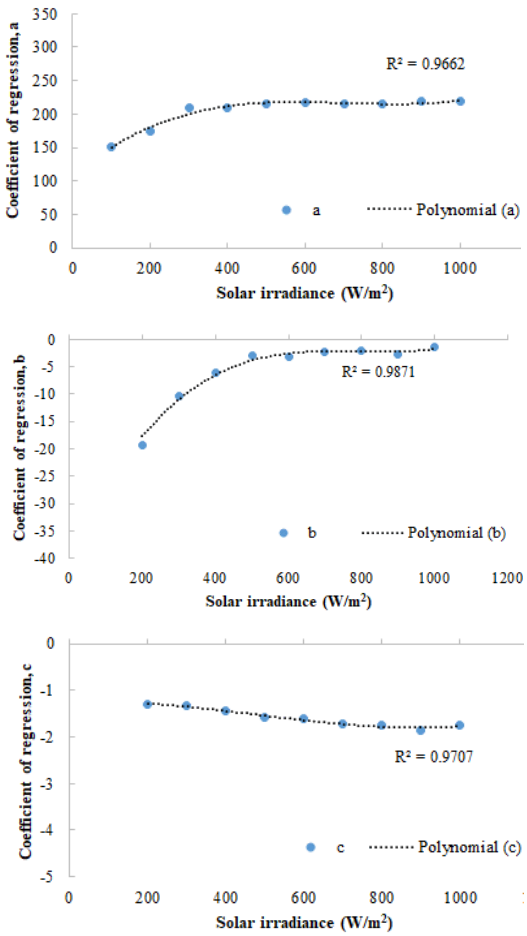


**Fig.10**. The relation between coefficient of regressions a, b, c and solar irradiance (G) for 1.74 $kW_p$ array power (without Boost Factor)

Likewise, the regression analysis was applied in order to find the relation between coefficients and irradiance. However, in this case, the third-order polynomial was taken to increase the accuracy of the models that have the general form as described by Eq. (2).

$$\begin{aligned} a\ G &= d + eG + fG^2 + hG^3 \\ b\ G &= i + jG + kG^2 + lG^3 \\ c\ G &= m + nG + oG^2 + pG^3 \end{aligned} \qquad (2)$$

The $R^2$ indicated in Figs. 9-12 show that most of regression lines were properly fit the data points. Then, substitution of Eq. (2) into Eq. (1) provides the flow rate as a function of water head and irradiance,

$$\begin{aligned} Q\ h,G\ &= m + nG + oG^2 + pG^3\ \ h^2 \\ &+ i + jG + kG^2 + lG^3\ \ h \\ &+ d + eG + fG^2 + hG^3 \end{aligned} \qquad (3)$$

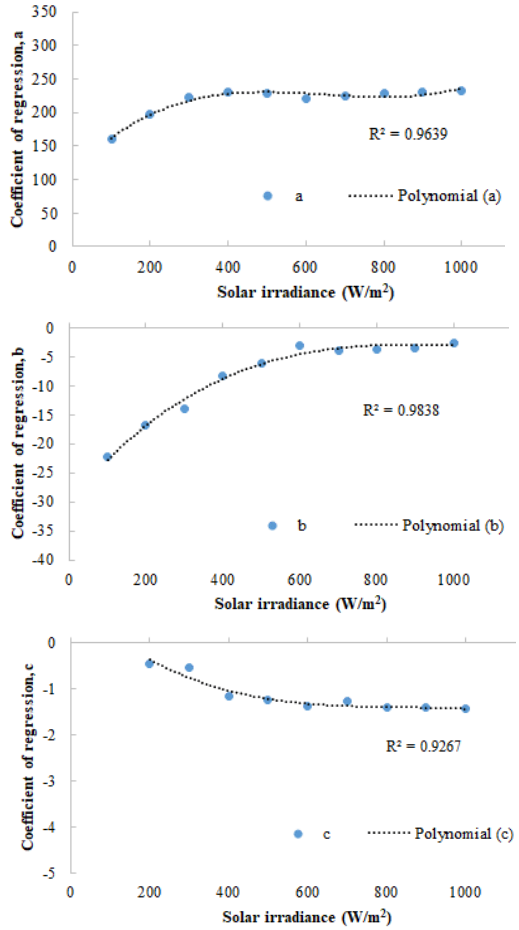


**Fig.11**. The relation between coefficient of regressions a, b, c and solar irradiance (G) for 1.74 $kW_p$ array power (with 1.05 boost factor)

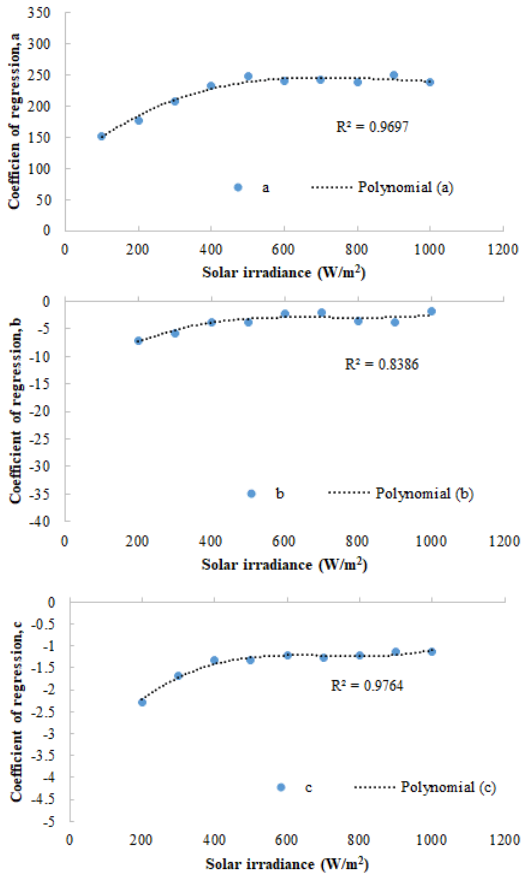


**Fig.12**. The relation between coefficient of regressions a, b, c and solar irradiance (G) for 1.74 $kW_p$ array power (with 1.1 boost factor)

## 4. Results and Discussion

### 4.1 Instantaneous flow rate

In order to estimate the daily water delivery, the proposed model described by Eq. (3) was used together with the daily irradiance profile to determine the instantaneous flow rate. As illustrated in Fig. 13, at any predefined head, the model provides a predicted flow rate as its output. Then, the instantaneous flow rate will be accumulated to determine the daily water delivery.

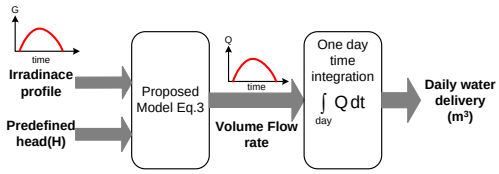


**Fig.13**. Estimation of daily water delivery based on proposed model

The PV pumping system was simulated by various irradiance profiles collected from pyranometer installed at Faculty of Engineering, Burapha University, Thailand. Furthermore, in the simulations, there are 3 different levels of water head. The 2-m of head represents the low head application while 5 m and 10 m represent moderate and high head respectively. However, it should be noted that the cut-in and cut-off irradiance are predefined at 50 $W/m^2$ in all cases.

Fig. 14 shows the result of instantaneous volume flow rate for 2.32 $kW_p$ array configuration obtained from the day in which the daily solar irradiance was 6.75 Peak Sun Hour (PSH). The water delivery curve is approximately flat profile throughout the day due to the oversizing of PV generation. The flow rate drop as a result of shadow cloud can be observed between 8:00 and 9:00 AM. The total water deliveries for this day were 165,

137 and 99 $m^3$/day for 2 m, 5 m and 10 m of head respectively.

The other example of irradiance profile was used in simulation and their results are illustrated in Fig. 15. This irradiance profile was collected in a rainy day that provides only 2 PSH daily irradiance. It can be seen that the instantaneous volume flow rate fluctuate for whole day as a result of significant irradiance swing. The total water delivery were 94, 56 and 17 $m^3$/day for 2 m, 5 m and 10 m of head respectively.

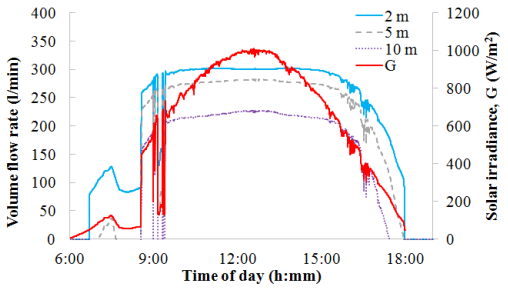


**Fig.14**. Volume flow rate and solar irradiance for 6.75 PSH in case of 2.32 $kW_p$ array power (without boost factor)

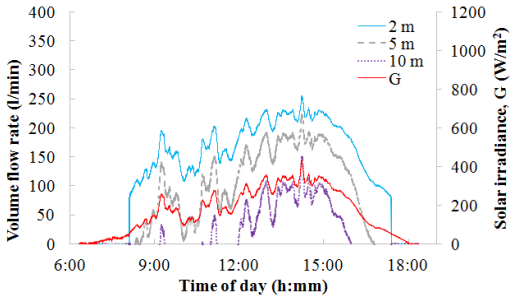


**Fig.15**. Volume flow rate and solar irradiance for 2.02 PSH in case of 2.32 $kW_p$ array power (without boost factor)

The model validation can be performed by comparing point by point between the simulation and the test results. For example, as seen in Fig. 14, at 5 m of pumping head and 1000 W/$m^2$ solar irradiance, the instantaneous flow rate predicted by model is 282 l/min while the test result (Fig. 5) indicates 280 l/min. In this condition, the error between model and test result is found to be less than 1%. This error trends to increase as irradiance decrease. The maximum error can be found less than 2% especially in low irradiance condition (<200 W/$m^2$). Therefore, the proposed model can be used to estimate the instantaneous water flow with insignificant error.

### 4.2 System efficiency

The capital costs of PV pumping systems depend mainly on PV array costs. The PV array including mounting is accounted for around 60-70% of total system costs. In economic point of view, the proper sizing of PV array installed in pumping system should be taken care. In many cases, oversized PV array will be ineffective to the pumping yield since the pump is operated far away from the best efficiency point (BEP). The typical head-flow characteristics of pump coupled to variable speed drive are exemplified in Fig. 16. For each pump speed, the BEP line intersects the pump performance curve at the different heads.

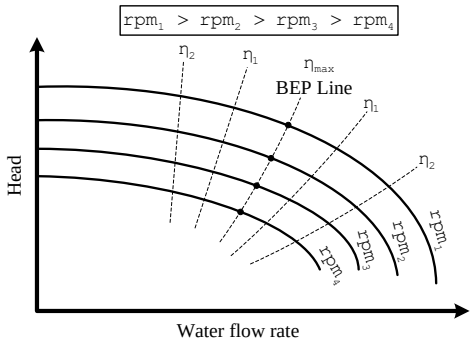


**Fig.16**. Typical centrifugal pump performance curves

The system efficiency were experimentally estimated at different solar irradiances and 2, 5 and 10 m of head when the pumping system was supplied from 2.32 $kW_p$ PV array as demonstrated in Fig. 17 (dash line). The system efficiency is calculated by

$$\eta_{sys} = \frac{P_{hyd}}{G\,A} = \frac{\rho g h Q}{G\,A} \qquad (4)$$

where $P_{hyd}$ is hydraulic power from pump (W), $A$ is PV array area ($m^2$), $G$ is solar irradiance ($W/m^2$), $\rho$ is water density ($kg/m^3$), and $g$ is gravity acceleration ($m/s^2$).

At low solar irradiance, low and medium head provide better system efficiency than high head. As irradiance exceeds 400 $W/m^2$, higher head provides higher system efficiency since each component operates near its best efficiency point. However, it can be observed that the system efficiency tends to gradually decrease according to the increasing of solar irradiance for all water heads. This reduction is due to the decreasing of PV and motor-pump efficiency as shown in Fig. 17 and Fig. 18 respectively.

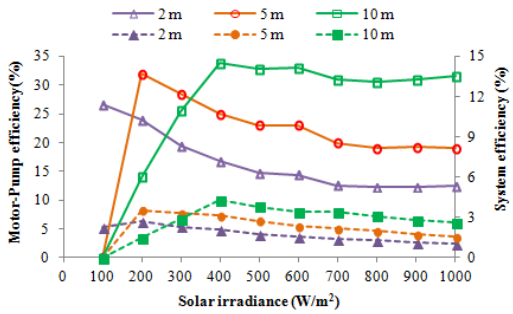


**Fig.17**. System efficiency for different solar irradiances at 3 different heads (2.32 $kW_p$ PV array)

The motor-pump efficiency is given by

$$\eta_{motor-pump} = \frac{P_{hyd}}{P_{inv}} \qquad (5)$$

where $P_{inv}$ is inverter output power (W).

The PV array efficiency is given by

$$\eta_{pv} = \frac{P_{pv}}{G\,A} \qquad (6)$$

where $P_{pv}$ is output power from PV array (W).

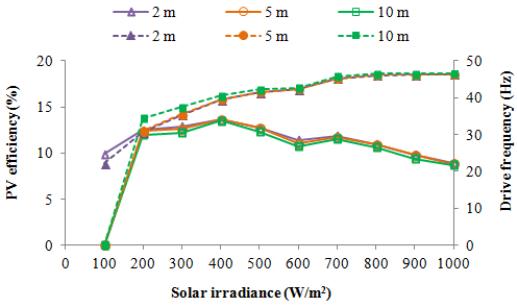


**Fig.18**. PV efficiency and drive frequency for different solar irradiances at 3 different heads (2.32 $kW_p$ PV array)

Fig. 18 illustrates the effect of solar irradiance on the drive frequency to which directly relates the pump speed. As expected, the increasing of solar radiation results in higher motor speed. Referring to Fig. 16, the change in motor speed causes the motor pump efficiency deviate to another value which can either be lower or higher than the one of the previous speed. Therefore, if the pump is operating at best efficiency point (BEP), further increasing in drive frequency (or pump speed) will reduce the pump efficiency. The experimental results depicted in Fig. 17 show that for each water head the BEP of pump was found at different irradiance. At 2 m head, the BEP occurs at 100 W/ $m^2$ which corresponds to 22 Hz of drive frequency while the BEP are shifted to the higher irradiance for higher head (5 m and 10 m). For all head, the drive frequencies are nearly constant when the irradiance exceeds 700 W/ $m^2$. This is due to limitation of drive frequency which strictly follows the V/F algorithm. Since the voltage at maximum power point of 2.32 $kW_p$ PV array is around 280 V, the drive frequency was then limited around 45 Hz.

The PV efficiency also affects to the system efficiency. Fig. 18 shows that the PV efficiency slightly decreases for irradiance higher than 400 W/ $m^2$. The reduction of PV efficiency is due to the increasing of PV cell temperature and the limitation of drive frequency as described previously.

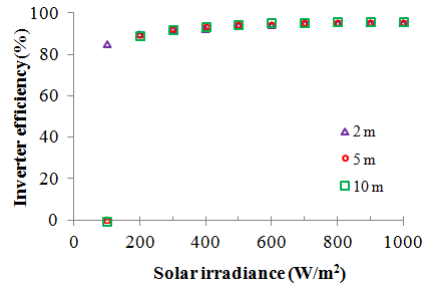


**Fig.19**. Inverter efficiency for different solar irradiances at 3 different heads (2.32 kWp PV array)

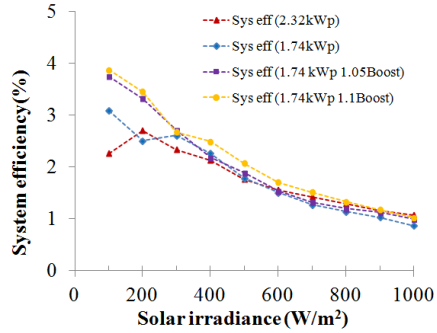


**Fig.20**. System efficiency for 4 different PV array configurations (2 m head)

The efficiency of an inverter indicates how much the DC power from array is converted to AC power supplied to motor. Therefore it relates only to the electric energy conversion. The inverter efficiency obtained from the test system is illustrated in Fig. 19. It can be observed that the inverter efficiency is almost constant at 95% for any heads while slightly increases due to higher power processing. For this reason, the effect of inverter efficiency on overall system efficiency can be neglected.

The system efficiencies for different PV array sizes are also considered. For a specific head, the different PV array sizes provide different

system efficiencies. Fig. 20 shows the comparison of system efficiency between PV pumping system supplied from 2.32 $kW_p$ (8 PV modules) and 1.73 $kW_p$ (6 PV modules) for 2 m head. At high irradiance, both array sizes provide almost the same system efficiency but it can be clearly seen the different of system efficiency for irradiance below 400 $W/m^2$. However, it is unable to decide which configuration exhibits higher system efficiency, and thus the average system efficiency $\bar{\eta}_{sys}$ which defined in Eq. (7) is proposed as an index.

$$\bar{\eta}_{sys} = \frac{\sum_{i=1}^{10} \eta_{sys,i} G_i}{\sum_{i=1}^{10} G_i} \qquad (7)$$

where $G_k = 100i\ W/m^2$ and $\eta_{sys,k} = \eta_{sys@G_k}$

Table 3 summarizes the average system efficiency for three heads and two PV array sizes. At low head, the same system efficiency are obtained for both array sizes but introducing of boost factor in case of smaller array size will improve the average system efficiency so that it provides higher efficiency than the larger array. For this reason, the smaller array size was an attractive choice in low head application since it provides higher efficiency, comparative daily water delivery, and lower cost.

**Table 3** Average system efficiency of PV pumping system for 3 different heads and 2 array sizes

| Head (m) | PV array size | | | |
|---|---|---|---|---|
| | **2.32 $kW_p$** | **1.73 $kW_p$** | **1.73 $kW_p$ (1.05 Boost)** | **1.73 $kW_p$ (1.1 Boost)** |
| 2 | 1.50% | 1.43 % | 1.54 % | 1.65 % |
| 5 | 2.21 % | 1.78 % | 2.08 % | 2.23 % |
| 10 | 3.06 % | - | 0.93 % | 1.84 % |

For moderate head, the pumping system supplied from 2.32 $kW_p$ array operates as efficient as the 1.73 $kW_p$ array with 1.1 boost factor. Due to the equality of system efficiency, it can be concluded that the daily water delivery will directly proportional to the PV array size. For high head, the larger PV array provides higher average system efficiency. The insufficient PV array will result in the extreme reduction of system efficiency as stated in [19].

### 4.3 Daily Water Delivery

The bar graphs shown in Figs. 21 – 24 present the daily water delivery for various system configurations. Figs. 21 and 22 illustrate the daily yield of pumped water for different PV array sizes without boost function. As expected, the daily water delivery gained from lower PV array power is less than the higher one. For 2 m head the smaller array size exhibit the same efficiency as the larger array so that their pumping yield per $kW_p$ of array are identical. However, this pumping yield per $kW_p$ can be enhanced by the boost factor. For 5 PSH, increase the PV array size from 1.74 $kW_p$ to 2.32 $kW_p$ will result in increasing of water delivery around 15%.

Table 4 summarizes the daily water pump for various conditions. At 5

m head and 2.32 $kW_p$ array (which is 2:1 ratio between PV array and motor-pump power), the pumping system can produce daily water delivery 50-60% extra than the 1.74 $kW_p$ array (ratio of 1.5:1).

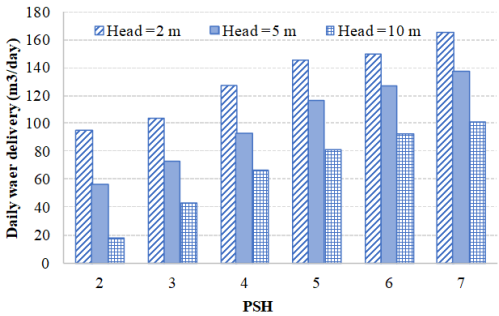


**Fig.21**. Daily simulated water delivery (2.32 $kW_p$ array, without boost factor)

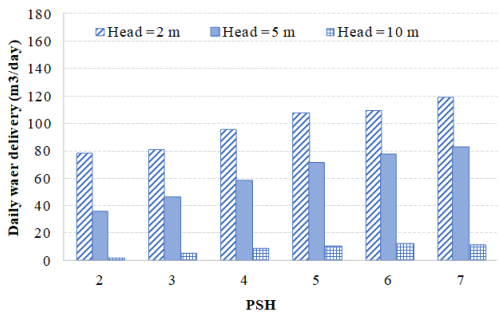


**Fig.22**. Daily simulated water delivery (1.74 $kW_p$ array, without boost factor)

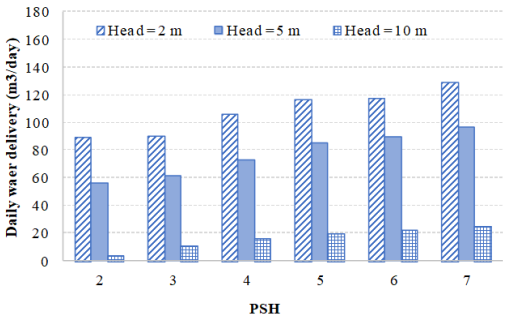


**Fig.23** Daily simulated water delivery (1.74 $kW_p$ array, with 1.05 boost factor)

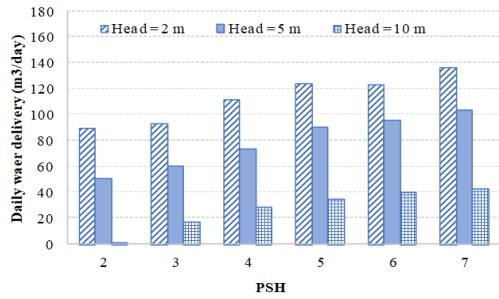


**Fig.24** Daily simulated water delivery (1.74 $kW_p$ array, with 1.1 boost factor)

It can obviously be seen from Table 4 that for high head application (10 m), the PV nominal power required for sufficient water delivered should be two times the motor-pump power. Hence, to configure the PV pumping system, the designer should optimize the sizing ratio depending on the required water delivery and water head. For example, in case of Thailand (Latitude 15.8700° N and Longitude 100.9925° E), the average peak sun hour is around 5 [20, 21] therefore for 5 m pumping head, the proper PV array power to meet the 100 $m^3$ of water consumption per day should be 2.32 $kW_p$ which is twice the pump power. In case of cost sensitive, the small array size can be used with an introducing of boost factor. Figs. 22 - 24 indicate how the boost factor affects the daily pumped water. For the same PSH and water head, it can be seen that the apparently augmentation of daily water delivery as a result of the increasing in motor speed. However, during the experiments, it can be observed that the large boost factor applied to pumping system can cause the motor to operate in overload situation.

**Table 4** The variation of daily water delivery with PSH and PV configurations

| PSH | 2.32 $kW_p$ array Without boost factor | | | 1.74 $kW_p$ array without boost factor | | | 1.74 $kW_p$ array with 1.05 boost factor | | | 1.74 $kW_p$ array with 1.1 boost factor | | |
|---|---|---|---|---|---|---|---|---|---|---|---|---|
| | Q ($m^3$/day) | | | Q ($m^3$/day) | | | Q ($m^3$/day) | | | Q ($m^3$/day) | | |
| | head | | | | | | | | | | | |
| | 2 m | 5 m | 10 m | 2 m | 5 m | 10 m | 2 m | 5 m | 10 m | 2 m | 5 m | 10 m |
| 2.02 | 94.69 | 56.75 | 17.14 | 78.36 | 37.91 | 0.06 | 88.88 | 56.57 | 4.53 | 89.74 | 53.31 | 4.24 |
| 2.93 | 103.56 | 72.56 | 42.46 | 81.21 | 47.37 | 4.68 | 90.16 | 61.30 | 11.06 | 93.04 | 61.45 | 19.77 |
| 3.99 | 127.32 | 92.42 | 64.80 | 95.43 | 58.77 | 7.71 | 105.47 | 72.73 | 16.45 | 111.30 | 74.03 | 30.94 |
| 5.01 | 145.85 | 115.68 | 79.50 | 107.66 | 71.75 | 8.42 | 116.39 | 85.09 | 19.88 | 123.78 | 90.66 | 35.84 |
| 6.29 | 149.96 | 126.86 | 90.61 | 109.19 | 77.54 | 9.26 | 117.49 | 89.80 | 22.91 | 122.87 | 95.66 | 38.10 |
| 6.75 | 165.47 | 137.28 | 99.37 | 119.08 | 82.94 | 8.47 | 128.70 | 96.70 | 24.81 | 136.11 | 102.90 | 40.62 |

## 5. Conclusion

The small-scale PV water pumping system was test and the empirical model based on the test results was obtained. This model was used to estimate the instantaneous flow rate for a given head and irradiance. The overall system and component efficiency are also collected from the experiment in order to investigate the performance for different system configurations. Finally, the daily water delivery for various peak sun hour and two different PV array configurations was evaluated. It can be summarized that for the area receiving 5 PSH solar irradiance (in the case of Thailand) and high head such as 10 meters, the PV array power should be twice the pump power in order to meet 80 $m^3$/day of water supply.

However, for lower head (2-5 m), the 1.5 times of PV array power to pump power can satisfy at least 100 $m^3$/day of water delivery. The oversized PV array is not necessary since its system efficiency will be lower than that of the optimum size PV array. In addition, the boost factor can greatly enhance approximately 20–30% the pumping performance without increasing PV array size.

The daily water delivery summarized in section 4.3 should be a design guideline for a pumping system similar to experimental system. A well-designed standalone PV pumping system decreases cost of PV equipment which makes it more interested in economic point of view and encourage the solar pump penetration.

## *References*

[1] Hrayshat, E.S.; Al-Soud M.S.; Li Z.; and Lu L. 2004. Potential of solar energy development forwater pumping in Jordan. *Renewable Energy* 29(8): 1393–9.

[2] Munir, A.; Al-Karaghouli, A.A.; and Al-Douri, A.A.J. 2007. A PV pumping station for drinkingwater in a remote residential complex. *Desalination* 209: 58–63.

[3] Djoudi Gherbi, A.; Hadj Arab, A.; and Salhi, H. 2017. Improvement and validation of PV motor-pump model for PV pumpingsystem performance analysis. *Solar Energy* 144: 310–320.

[4] Jafar, M. 2000. A model for small-scale photovoltaic solar water pumping. *Renewable Energy* 19: 85–90.

[5] Adelmalek Mekeddem; Abdelhamid Midoun; Kadri, D.; Said Hiadrsi; and Iftikhar A. Raja. 2011. Performance of a directly-coupled PV water pumping system. *Energy Conversion and Management* 52: 3089–3095.

[6] Ghoneim, A.A. 2006. Design optimization of photovoltaic poweredwater pumping systems. *Energy Conversion and Management* 47: 1449–1463.

[7] Benghanem, M.; Daffallah, K.O.; Alamri, S.N.; and Joraid, A.A. 2014. Effect of pumping head on solar water pumping system. *Energy Conversion and Management* 77: 334–339.

[8] Protogeropoulos, C. and Pearce, S. 2000. Laboratory evaluation and system sizing charts for a second generation direct PV-powered, low cost submersible solar pump. *Solar Energy* 68 (5): 453–474.

[9] Short, T.D. and Burton, J.D. 2003. The benefits of induced flow solar powered water pumps. *Solar Energy* 74: 77–84.

[10] Mona, N. Eskander and Aziza M. Zaki. 1997. A maximum efficiency photovoltaic-induction motor pump system. *Renewable Energy* 10 (1): 53–60.

[11] Aziza M. Zaki and Mona, N. Eskander. 1996. Matching of photovoltaic motor–pump systems for maximum efficiency operation. *Renewable Energy*, 7 (3): 279-288.

[12] Betka, A. and Moussi, A. 2004. Performance optimization of a photovoltaic induction motor pumping system. *Renewable Energy* 29(14): 2167-2181.

[13] Taha, M.S. and Suresh, K. 1996. Maximum power point tracking inverter for photovoltaic source pumping applications. In *Proceeding of International Conference on Power Electronics, Drives and Energy Systems for Industrial Growth*. India, 8–11 Jan 1996. Vol.2: 883–886.

[14] Abdel-Karim Daud and Marwan M. Mahmoud. 2005. Solar powered induction motor-driven water pump operating on a desert well, simulation and field tests. *Renewable Energy* 30(5): 701–714.

[15] Benlarbi, K.; Mokrani, L.; and Nait-Said, M. 2004. A fuzzy global efficiency optimization of a photovoltaic water pumping system. *Solar Energy* 77(2): 203–216.

[16] Arab, A.; Chenlo, F.; and Benghanem, M. 2004. Loss-of-load probability of photovoltaic water pumping systems. *Solar Energy* 76(6): 713–723.

[17] Rungsiyopas, M.; and Chuenwattanapraniti, C. 2017. Effect of installed photovoltaic array capacity on the performance of surface pumping systems. *Journal of Research and Applications in Mechanical Engineering* 5(2): 82–93.

[18] Benghanem M.; Daffallah K.O.; and Almohammedi A. 2018. Estimation of daily flow rate of photovoltaic water pumping systems using solar radiation data. *Results in Physics* 8: 949-954.

[19] Argaw N. 1995. Photovoltaic water pumps coupled with DC/AC inverter. *International Journal of Solar Energy* 18(1): 41-52.

[20] Department of Alternative Energy Development and Efficiency, Ministry of Energy. 2009. The solar radiation map. Bangkok: Department of Alternative Energy Development and Efficiency, Ministry of Energy.

[21] Janjai, S.; Laksanaboonsong, J.; Nunez, M.; and Thongsathitya, A. 2005. Development of a method for generating operational solar radiation maps from satellite data for a tropical environment. *Solar Energy* 78(6): 739–751.

## Authors' Biography:

Dr.Montana Rungsiyopas is a lecturer of mechanical engineering at Department of Mechanical Engineering, Burapha University. Her research interests are thermal systems, energy technology and applications.

Asst. Prof. Dr.Chokchai Chuenwattanapraniti is an assistant professor of electrical engineering at Department of Electrical Engineering, Burapha University. His research interests are power electronics applications and photovoltaic systems.